LIKE EARLY STARVATION 1 interacts with amylopectin during starch biosynthesis

Short title: Specificity of ESV1 and LESV for starch glucans

Rayan Osman[1], Mélanie Bossu[1], David Dauvillée[1], Corentin Spriet[1,2], Chun Liu[3], Samuel C, Zeeman[3], Christophe D'Hulst[1] and Coralie Bompard[1,*]

[1]Université de Lille, CNRS, UMR 8576 - UGSF - Unité de Glycobiologie Structurale et Fonctionnelle, Lille, France

[2]Univ. Lille, CNRS, Inserm, CHU Lille, Institut Pasteur de Lille, US 41 - UAR 2014 - PLBS, F-59000 Lille, France

[3]Institute of Molecular Plant Biology, ETH Zurich, Universitätstrasse 2, 8092 Zurich

[*]Corresponding author: Coralie Bompard (C.B) coralie.bompard@univ-lille.fr

The author responsible for distribution of materials integral to the findings presented in this article in accordance with the policy described in the Instructions for Authors (https://academic.oup.com/plphys/pages/General-Instructions) is C.B.

Abstract

Starch is the major energy storage compound in plants. Both transient starch and long-lasting storage starch accumulate in the form of insoluble, partly crystalline granules. The structure of these granules is related to the structure of the branched polymer amylopectin: linear chains of glucose units organized in double helices that align to form semi-crystalline lamellae, with branch points located in amorphous regions between them. EARLY STARVATION 1 (ESV1) and LIKE EARLY STARVATION 1 (LESV) proteins are

involved in the maintenance of starch granule structure and in the phase transition of amylopectin, respectively, in Arabidopsis (*Arabidopsis thaliana*). These proteins contain a conserved tryptophan-rich C-terminal domain folded into an antiparallel β-sheet, likely responsible for binding of the proteins to starch, and different N-terminal domains whose structure and function are unknown. In this work, we combined biochemical and biophysical approaches to analyze the structures of LESV and ESV1 and their interactions with the different starch polyglucans. We determined that both proteins interact with amylopectin but not with amylose and that only LESV is capable of interacting with amylopectin during starch biosynthesis. While the C-terminal domain interacts with amylopectin in its semi-crystalline form, the N-terminal domain of LESV undergoes induced conformational changes that are probably involved in its specific function of mediating glucan phase transition. These results clarify the specific mechanism of action of these two proteins in the biosynthesis of starch granules.

Introduction

In plants, starch accumulates as water-insoluble, partly crystalline granules. In leaves, transitory starch accumulates in chloroplasts during the day and is used as carbon and energy source during the night. In heterotrophic tissues, storage starch accumulates over longer time frames and fuels germination or seasonal regrowth. Starch granules are made up of two polymers of glucose residues, namely amylose and amylopectin that adopt different 3D structures (for review (Pfister and Zeeman, 2016)). and have different physicochemical properties. They are organized as α-1,4-glucans linked one to another by α-1,6-bonds (= branching points). The major polyglucan of starch is amylopectin (70-80% of the starch content) which is organized by alternating regions containing linear chains or branching points while amylose is poorly branched (<1% α-1,6 bonds)(Pérez and Bertoft, 2010; Pfister and Zeeman, 2016).

Amylopectin is synthesized by the concerted activities of soluble starch synthases (SSs), starch branching enzymes (SBEs) and starch debranching enzymes (SDBEs) acting independently or in concert, in particular by forming transient complexes during the various stages of biosynthesis (Crofts et al., 2015). Soluble SSs transfer the glucose residue of ADP-Glucose (the precursor molecule) to the non-reducing end of an elongating glucan (Larson et al., 2016; Xie et al., 2018). Branching points are introduced by SBEs which cleave an α-1,4

bond of a pre-existing glucan and transfer the malto-oligosaccharide located toward the non-reducing end onto a neighboring glucan or onto another part of the cleaved glucan, forming an α-1,6 bond (Sawada et al., 2014). The isoamylase class (ISA1) of DBEs are involved in the synthesis of amylopectin by hydrolyzing the excess and incorrectly positioned α-1,6 bonds of the nascent, soluble amylopectin molecule to optimize the branching pattern and facilitate amylopectin crystallization (Ball et al., 1996; Myers et al., 2000; Delatte et al., 2005; Wattebled et al., 2005). The inactivation of ISA1 in the plant induces the accumulation of phytoglycogen (an abnormal soluble glucan so-called because of some similarity to glycogen structure) and alters the structure of the residual insoluble starch, which depends on the pattern of branching points and linear chains (Zeeman et al., 1998; Delatte et al., 2005; Wattebled et al., 2005; Pfister et al., 2014). Prior to the discovery of LESV and while certain forms of insoluble altered amylopectin are still present in the *isa1* mutant plants, it was widely assumed that the starch granule matrix formation involves self-organization physical process events during the early stages of granule formation (Waight et al., 2000; Ziegler et al., 2005) following the action of ISA1 (Zeeman et al., 1998; Delatte et al., 2005; Wattebled et al., 2005; Streb et al., 2008).

Within amylopectin, the entwining of adjacent chains into double helices gives rise to both secondary and tertiary structures of the molecules. These structures align and pack into dense, crystalline lamellae, which alternate with amorphous lamellae that contain most branching points and chain segments connecting the crystalline lamellae. The resulting regular alternating pattern of crystalline and amorphous layers is a feature of all wild type starches, and is believed to underlie the frequently observed 9-10 nm repeat structure (Buleon et al., 1998).

EARLY STARVATION 1 (ESV1) and LIKE EARLY STARVATION 1 (LESV) have been described to be involved in starch granule stabilization and phase transition of amylopectin molecules from soluble to crystalline form in starch granules, respectively (Feike et al., 2016; Liu et al., 2023). ESV1 and LESV were discovered in starch from Arabidopsis leaves and potato (*Solanum tuberosum*) tuber, but the genes are conserved across the plant kingdom and the orthologous proteins were present in starches of cassava, maize and rice (Feike et al., 2016; Helle et al., 2018). The implication of ESV1 and LESV in starch metabolism has been demonstrated after the analysis of KO mutant lines of *Arabidopsis* in which the starch phenotype has been specifically altered (Feike et al., 2016; Liu et al., 2023). Mutant *esv1*

plants show a phenotype in which the diel cycle of transitory starch metabolism is altered and carbon reserves are abnormally exhausted too early before dawn. In contrast, mutant *lesv* plants accumulate phytoglycogen beside insoluble starch granules, especially when initiating starch synthesis *de-novo*. Complementation experiments have shown that over-expression of LESV in ISA1-deficient plants or yeast (*Saccharomyces cerevisiae*) cells induces the phase transition of amylopectin, even though it has not been subjected to the action of DBEs. Over-expression of ESV1 in an ISA1-deficient background, while inducing the production of minute amounts of insoluble glucans, is not as effective as LESV. However, ESV1 overexpression in a wild-type background induces a high accumulation of insoluble starch. These results have been interpreted to mean that LESV is involved in the phase transition of amylopectin, while ESV1 stabilizes starch granules, protecting them from premature digestion (Liu et al., 2023).

Protein sequence analysis of ESV1 and LESV failed to identify already known catalytic or functional domains (Feike et al., 2016). ESV1 and LESV share a conserved domain of about 240 amino acids located at their C-termini. Their N-terminal regions are of different lengths (130 amino- acids in ESV1 and 304 in LESV including the plastid localization signal peptide) and do not share sequence homology to each other. The C-terminal domains contain numerous Tryptophan and aromatic amino acid residues organized in conserved repeated motifs also containing acidic amino acids, *i.e.* aspartic acid and glutamic acid residues. The presence of these repeated motifs could constitute binding sites for numerous glucans or mediate interaction with long glucans such as starch components (Feike et al., 2016). Both proteins were recently investigated by a combination of structural and functional studies (Liu et al., 2023). The structures of ESV1 and LESV were modeled using Alphafold2 (Jumper et al., 2021), complemented by biophysical approaches (Liu et al., 2023). The results showed a unique and common fold for the conserved C-terminal domain. The tryptophan-rich regions of both ESV1 and LESV proteins have been predicted with high confidence, to fold into an extended planar β-sheet. Localizing the conserved motifs of aromatic and acidic residues within these predicted structures revealed that they align into linear stripes regularly spaced and running across both sides of the β-sheet, perpendicular to the β-strands. The aromatic stripes are about 70 Å long and distance between them is about 14 Å, which corresponds well to the lengths and spacing, respectively, of the double helices of amylopectin in the crystalline phase of starch granules (Buleon et al., 1998). It has been proposed that this domain constitutes a previously uncharacterized carbohydrate binding

surface capable of binding at least two double helices of amylopectin molecule on each side of the β-sheet. Synthetic biology approaches in yeast and *in-vivo* experiments in *Arabidopsis*, provide direct evidence that LESV is directly involved in promoting the phase transition of amylopectin. To do that, the described carbohydrate binding surface would allow LESV to bind several double helices of amylopectin, thereby promoting their organization and transition from a soluble to a crystalline phase. This domain would allow ESV1 to maintain the organization of glucans in newly-formed granules and to limit their enzymatic degradation during the daytime phase (Liu et al., 2023). Thus, while the two proteins share a domain that enables them to bind to ordered double-helices of amylopectin, they appear to have different functional roles in the cell. Their N-terminal domains, which are not conserved and whose structure is unknown, could be at the origin of these differences and may modulate polyglucan binding or interactions with other protein partners during starch biosynthesis.

Interestingly, *in-vitro* studies of the affinity of the two proteins for starch polyglucans have suggested that ESV1 interacts with amylopectin but not LESV, which binds only amylose (Malinova et al., 2018; Singh et al., 2022). This latter result is inconsistent with the results of Liu et al. (Liu et al., 2023) which show that LESV intervenes in the structuring of amylopectin molecules to form starch granules and should be able to interact with amylopectin. In an attempt to resolve this ambiguity, and further elucidate the mechanism of action of these proteins, we studied in the interaction of ESV1 and LESV with α-polyglucans using a combination of biochemical, biophysical and structural approaches. Our aim was first to determine the affinity of the two proteins for the different polyglucans and to identify differences that would allow to clarify their function in the plant. As the N-terminal domains of ESV1 and LESV may be involved in the function of each of the two proteins, we also carried out a structural and biophysical study to analyze their potential involvement in the interaction with polyglucans. Our results show that ESV1 and LESV both interact with amylopectin, but not with amylose. They further show that this interaction involves conformational changes in the N-terminal domain of LESV. Thus, this domain is also likely involved in the specific recognition of amylopectin by LESV during starch biosynthesis, supporting the idea that it acts upstream of ESV1 in the pathway.

Results

The N-terminal domain of LESV contains helices whose folding and position depend on protein environment

C-terminal domain shared by ESV1 and LESV has an original structure that exhibits the characteristics required for the binding of long polyglucan chains (Liu et al., 2023). However, both proteins have an N-terminal domain, longer in LESV, whose function is not yet defined and for which Alphafold2 does not have a reliable structure prediction.

To go beyond the Alphafold2 models available for LESV and ESV1, we recalculated a set of five Alphafold2 models for both proteins. Specifically, we calculated in-house the templates for the constructs used in the CD and SAXS experiments (Liu et al., 2023). The predicted regions with a high degree of confidence (pLDDT > 90) for ESV1 (amino acids from 142 to 395) and LESV (amino acids from 318 to 573) remain identical in the 5 models (Liu et al., 2023) (Figure 1A) which suggests a high stability for this domain. In these models, we were interested in the predicted structures of the less conserved domains. The regions close to the C-terminal β-sheet of ESV1 (46 amino acid residues at the N-terminus and the polyproline region at the C-terminus), which are poorly conserved between species, are predicted to be disordered. In the C-terminal region of the β-sheet, located on one of its faces (Face A, Figure 2), a short α-helical region (residues 378 to 395) is predicted with a high degree of confidence for its structure and position relative to the β-sheet. This helix is also present in LESV (residues 555 to 578) with the same degree of confidence.

The structure of the N-terminal region of LESV is predicted with low to very low confidence. However, it has been shown that three helical regions located in an island of conservation are predicted with pLDDT >70 (Liu et al., 2023). Only one of these forms a long helix (residues 245 to 273) whose position relative to the β-sheet, is predicted with high confidence on the Face A of the β-sheet (Figure 1A). It is predicted with the same confidence in all models generated by Alphafold2, but its position may vary from one model to another, suggesting that it may be modified according to the protein's environment. For other helices, although predicted with pLDDT > 70, their size and positions are not equivalent between models. This result indicates that the N-terminal domain of LESV is probably mainly disordered and susceptible to induced helix folding depending upon the conditions.

We analyzed the structure of the Face A of the β-sheet of ESV1 in the region equivalent to that occupied by helix 245-273 on LESV (Figure 2). Alphafold2 does not predict a long helix at this location, but a loop (amino acids 109 to 138) with a pLDDT> 70 and an expected positional error < 3 Å (Figure 2). The helix in LESV and loop in ESV1 are stabilized by numerous interactions with the amino acids of the β-sheet in both proteins, including some of the conserved aromatic and acidic residues that cover half the height of the sheet. These two structures are located on the same side of the β-sheet as the short, C-terminal helices conserved in both proteins. Their presence in this configuration is not compatible with the binding of the amylopectin double helices, potentially resulting in a polarity in the glucan-binding domain: one side is accessible, the other is not.

The N-terminal domain of LESV is partially disordered and folds close to the tryptophan rich domain

The two proteins have different functions within the plant and we hypothesized that this difference might be related to their differing N-terminal domains. These domains are predicted to have rather dynamic structures – a property incompatible with structural analysis by X-ray crystallography. Therefore, we investigated their structures using a combination of more appropriate biophysical approaches such as circular dichroism and SAXS.

SAXS is an X-ray scattering approach for proteins in solution. While this approach does not provide high resolution structure, it allows the analysis of the molecular envelope and the position of protein domains in relation to each other. If the structure of one domain is known, it can be used to position and model *ab initio* the structure of the missing part, which can be crucial in studying the function of a dynamically structured protein. We used SAXS to analyze the structure and position of the N-terminal domain of LESV, as that of ESV1 is extremely short.

In order to visualize and localize the N-terminal domain of LESV, we performed an *ab initio* modelling based on the structure of the high-resolution C-terminal domain model given by Alphafold2 and the SAXS data (Liu et al., 2023). The result obtained for LESV is shown in Figure 1B. The obtained model, which fits the SAXS data with a high degree of confidence (χ^2= 3.8) **(**Figure 1C), shows that the end of the C- and N-terminal domains (between 50 and 80 residues) are rather disordered and emerge from the overall structure, while the rest of the domain is organized around or close to the β-sheet. The presence of this domain around, or at

least close to, the β-sheet is likely to affect glucan-binding and could contribute to the differences in function between the two proteins described in (Liu et al., 2023).

ESV1 and LESV interact differently with α-1,4-linked glucose polymers

The structural polydispersity of amylose and amylopectin solutions, as well as their high viscosity, precluded their use in conventional structural biology approaches (SAXS or X-ray crystallography) or SPR. To clarify the specificities of ESV1 and LESV and their interaction with starch glucans, we performed EMSA experiments which are better suited to the biochemical properties of glucans. EMSA is a rapid and sensitive method to detect protein-glucan interactions. It is based on the observation that the electrophoretic mobility of a protein can be retarded in polyacrylamide gels containing increasing concentrations of a ligand, leading to a shift in the position of the protein band. In case of specific affinity, the intensity of this shift will be proportional to the concentration of glucan in the gel. First, we followed the influence of increasing concentrations of amylose or amylopectin on the electrophoretic mobility of LESV and ESV1 (Figure 3). On native polyacrylamide gels containing 0.1 and 0.3% (w/v) amylopectin, both ESV1 and LESV show a large reduction in mobility which increased with amylopectin concentration (Figure 3A) demonstrating a strong affinity of the two proteins for this polysaccharide.

In contrast, no electrophoretic mobility differences were found for LESV and ESV1 in native gels containing amylose in the same concentration range, suggesting that LESV and ESV1 have no affinity for amylose under the tested conditions (Figure 3B). Amylose contains longer chains than amylopectin and much fewer branching points. Next, we decided to test the affinity of LESV and ESV1 for glycogen (a highly branched α-linked glucans) (Figure 3C). Two different final concentrations of glycogen (0.25 and 1% w/v) were added to 8% (w/v) acrylamide native gels. A shift to lower mobility of the LESV protein band was observed in the gel containing 0.25% (w/v) glycogen compared to the reference protein band. This shift is accentuated when the glycogen concentration is increased, suggesting here again that LESV has specific affinity for this branched glucan. Interestingly, ESV1 did not show any change in its electrophoretic mobility in the presence of glycogen, eliminating a potential affinity of ESV1 for glycogen.

Binding of amylopectin to LESV causes α-helices to appear in the N-terminal domain of the protein

In order to better characterize the mode of interaction of ESV1 and LESV with glucans, the role of N-terminal domains, and to highlight conformational changes of the proteins' structure during complex formation, we performed an SR-CD study. CD is the method of choice for analyzing the structure of a protein by visualizing its content in secondary structural elements. It also allows the study of interactions between proteins and their ligands, especially when the latter lead to protein structural changes. SR-CD extends the limits of typical CD spectroscopy by providing an extended spectral range, improving signal-to-noise ratio and enabling faster data acquisition (Hussain et al., 2012; Hussain et al., 2018). Quantitative analysis of CD spectra also makes it possible to predict the secondary structure content of a protein.

We compared the spectra obtained for the proteins alone and in presence of amylopectin and amylose as the latter doesn't interact with the proteins. The CD spectra of both proteins alone have been described in (Liu et al., 2023) and show that they are structured albeit with differences in the secondary structure composition (Figures 4 and Figure 5). For ESV1, the pattern of CD spectra corresponds to a folded protein with a strong positive band at λ=196 nm and only one negative band at λ=220 nm, which are characteristic of proteins containing mainly β-strands/sheets. For LESV, the pattern of the spectrum reveals a global folding of β-strands and α-helices. Indeed, the LESV CD spectrum shows a strong maximum at λ=192 nm and a minimum at λ=216 nm, which are the signature of the presence of β-structures, but unlike ESV1, the spectrum also shows two shoulders at λ=210 and λ=222 nm, which is evidence for the additional presence of α-helices (Liu et al., 2023).

To analyze the structural effect of interactions between the ESV1 and LESV proteins and amylopectin, solutions of each protein were mixed with 1% (w/v) amylose or 1% (w/v) amylopectin solutions prior to measurement. For each spectrum, the composition of the secondary structure elements was determined using BestSel (Micsonai et al., 2015). The values obtained were compared with those obtained for the proteins alone.

Figure 4 shows the superposition of the spectra of ESV1 alone and added to amylopectin or amylose solutions. The analysis shows broadly equivalent spectra for ESV1 in the presence of amylose or amylopectin, with a degree of structuring that appears to be slightly lower for the protein alone. Analysis of the composition of secondary structural elements has been performed using BestSel (Figure 4, inset). BestSel is a tool that allows the secondary

structure determination and fold recognition from protein circular dichroism spectra. It indicates an equivalent composition for ESV1 alone or in the presence of amylose and a slight reduction or modification of some strands and α-helices when the protein is in the presence of amylopectin. This result indicates that ESV1 interacts with amylopectin without undergoing conformational changes in the protein. This result demonstrates that the C-terminal domain, which constitutes the vast majority of ESV1, does not undergo a conformational change following interaction with amylopectin.

The same analysis was performed for LESV (Figure 5). The spectrum obtained for the LESV/amylopectin mixture shows peaks of much higher magnitude than those obtained for the protein alone or in the presence of amylose. The positive peak at λ=192 nm has a magnitude 60% higher than that of the protein alone, indicating a higher structuring of the protein. At λ=208 and λ=215 nm, the molar ellipticity values indicating the presence of α and β structures, are 50% lower than those observed for the protein alone or in the presence of amylose. More interestingly, the molar ellipticity at λ=222 nm, indicating the presence of α-helices, is much lower (70%) than that observed for the protein alone or in the presence of amylose. This result shows that the binding of amylopectin induces a conformational change of LESV notably through the formation of additional α-helices upon binding of amylopectin.

To identify and quantify the conformational changes undergone by LESV in the presence of amylose and amylopectin, the composition of the secondary structural elements was analyzed using BestSel (Micsonai et al., 2015). The results (Figure 5, inset) confirm the analysis of the CD spectra: the composition of the β-strands and turns is equivalent whether LESV is alone or in the presence of amylose or amylopectin, likely indicate that the structure of the β-domain is not modified by the presence of polyglucans. The high conservation observed in the C-terminal domain of both LESV and ESV1 supports the hypothesis that the lack of conformational change in the ESV1 C-terminal domain upon amylopectin binding confirms this hypothesis. A higher number of α-helices is observed when LESV is in the presence of amylopectin. This confirms that LESV interaction with amylopectin induces the formation of α-helices, presumably within the N-terminal domain, with the structure of the C-terminal domain remaining unchanged.

The spectrum obtained for the LESV/amylose mixture had a broadly similar appearance to that of LESV alone, with peaks of slightly lower magnitude confirming EMSA experiments

showing no affinity for this glucan. LESV in the presence of amylose seems to have a slightly lower number of α-helices and strands than the protein alone. This result suggests that although LESV does not interact with amylose, the presence of high amounts of amylose may slightly modify the behavior of the protein in solution.

Amylopectin binding affects the melting temperature (TM) of LESV but not that of ESV1

Enhanced detection of ligand binding can be achieved through thermal denaturation studies monitored by SR-CD. This method is more sensitive than simple spectral differences as it can detect interactions that do not induce structural modifications of the proteins. The experiment involves measuring the CD spectrum of proteins at different temperatures alone or in presence of ligand. Increasing the temperature causes progressive denaturation of the protein and therefore a change in the molar elipticity. These changes can be used to monitor denaturation at a given wavelength and estimate the mixing temperature (TM). As the presence of a ligand generally tends to stabilize the protein, its TM will be higher in the presence of the ligand.

The CD signal variation was measured as a function of the temperature for both proteins, alone and in the presence of amylopectin, under the same conditions as for the spectra at constant temperature. Figure 6A, 6B, 6C, 6D present the different spectra obtained for LESV and ESV1 during the temperature gradient. To assess the impact of the presence of amylopectin on LESV and ESV1 stability, we measured the TM of the mixtures by monitoring the molar ellipticity evolution as a function of temperature at λ=195 nm and λ=190 nm respectively. The curves obtained have been normalized and are presented in Figure 6E, 6F. The experiment shows that the denaturation of LESV is slowed down in the presence of amylopectin as the TM increases dramatically from 55° to 65°. Thus, the presence of amylopectin stabilizes LESV, attesting to a strong interaction. The denaturation curves for ESV1 show the same pattern and can be overlaid with an inferred TM of about 50°C for ESV1. Therefore, in contrast to LESV, the binding of amylopectin does not affect the thermostability of ESV1.

ESV1 and LESV accumulate on the entire surface of starch granules.

Having demonstrated the interaction between ESV1 and LESV in solution, we investigated whether the proteins are also able to bind amylopectin in its insoluble form. To do that, the binding of ESV1 and LESV to starch granules was monitored by UV fluorescence microscopy. This approach, visualizes proteins via the fluorescence of their aromatic residues without adding any external probe, and has already been used to visualize proteins on starch granules (Tawil et al., 2011). To visualize only ESV1 and LESV, we used starch granules from Waxy maize that has no GBSS protein present in the starch granules (GBSS is the major granule-bound protein). Thus, the fluorescence of the granules could be distinguished from the fluorescence of the protein being studied (see Materials and Methods). The measurement was carried out simultaneously in visible light, to visualize starch granules, and with excitation at λ=310 nm, which allows the tryptophan residues to be excited, to visualize proteins (Figure 7). The emission spectrum was obtained using a filter to select a wavelength range between 329 and 351 nm which is specific to tryptophan residues. Two controls were carried out, the first with starch granules alone to verify the absence of fluorescence and the second with starch granules incubated with bovine serum albumin (BSA) to verify the absence of unspecific protein binding. When starch granules were incubated with ESV1 or LESV proteins, the tryptophan fluorescence images revealed a distinct halo over the surface of the starch granules, demonstrating the affinity of the proteins for amylopectin in its insoluble, semi-crystalline form. However, the intensity of the fluorescence seemed to be greater in the case of ESV1 particularly on larger granules. This could be interpreted as ESV1 having a greater affinity than LESV for amylopectin in its insoluble form.

The C-terminal tryptophan rich domain of ESV1 and LESV can bind two double helices of amylopectin (at least) on one face of the β-sheet

To gain more insight into the binding of ESV1 and LESV to insoluble amylopectin, we simulated the interaction between the C-terminal domain of the proteins and two double helices of amylopectin. To do this, we used the model of LESV containing the β-sheet and the conserved and well positioned α-helix described in (Liu et al., 2023) and shown in Figure 1. Since in both proteins, one side of the C-terminal β-sheet may be partially obscured (by the long helix in LESV, and the long loop in ESV1; Figure 2), we only studied the interaction of

amylopectin on the accessible side of the β-sheet. For the docking simulation, the parts of the N-terminal domain other than the conserved, well positioned α-helix were omitted

We first performed a docking calculation with one molecule of protein and one double helix of amylopectin centred on one aromatic stripe of LESV on the accessible face of the β-sheet. We obtained a good solution in which the amylopectin double helix binds the β-sheet, aligning well with the aromatic stripe. We repeated the same approach with the protein binding a second amylopectin double helix as the target centred on the second aromatic stripe. We again obtained a solution shown in Figure 8. On this structure, two double helices of amylopectin bind along the aromatic stripes and lie parallel to each other separated by 10 Å (between the axis of the double helices). This arrangement of the double helices in relation to each other corresponds to the arrangement of the amylopectin molecules described for starch (Imberty et al., 1988). This result suggests that the conserved C-terminal domain conserved of ESV1 and LESV is perfectly suited for the interaction of the proteins with the insoluble form of native amylopectin, or for helping that structure to form.

The amylopectin molecules interact with the protein domain through numerous interactions typical of protein-sugar interactions, as predicted from the analysis of the primary sequence of the β-sheet domain and the distribution of conserved amino acids in the Alphafold2 model (Figure 8). The glucose rings interact by hydrophobic stacking with the aromatic rings of the β-domain all along the double helices. The acidic residues conserved in LESV and ESV1 also play an important role in the interaction by participating in hydrogen bonding with the hydroxyl groups of the glucose residues on the sides of the double helices. On face A, described above, there is an analogous organization in stripes of aromatic and acidic residues, suggesting that double helices could also bind on this face, possibly after structural reorganization of the conserved helix (LESV) or loop (ESV1) allowing both sides of the proteins to interact with amylopectin molecules.

Discussion

ESV1 and LESV bind specifically to amylopectin.

In this work, we investigated the interaction specificities of ESV1 and LESV with the different components of starch. The properties of amylopectin and amylose macromolecules, which are complex, non-homogeneous and often dense glucans in solution, limited the

approaches that could be used. Previous work on the affinity of ESV1 and LESV for starch components (Malinova et al., 2018; Singh et al., 2022) focused on the interaction between ESV1 and LESV and starch glucans in insoluble form and/or on different mutant starch granules. That work proposed that ESV1 and LESV interact with starch granules, each having specific affinity for amylopectin or amylose respectively, with affinity being independent of the protein/glucan ratio. Those results are, however, not fully consistent with the recent characterization of LESV and ESV1 (Liu et al., 2023), nor with the results presented here. First, we chose an EMSA approach, which allowed us to analyze the behavior of both proteins in relation to each of the polyglucans. The migration profile of the two proteins shows that both proteins have a strong affinity for amylopectin and that this affinity increases with the amount of this glucan, attesting to their specificity. Conversely, in the presence of amylose, we did not observe any migration retardation associated with amylose. Second, structural analysis of ESV1 and LESV in the presence of amylose and amylopectin by SR-CD shows that only the presence of amylopectin induces conformational changes in LESV upon interaction, leading to the structuring of disordered regions of the N-terminal domain of the protein into α-helices. No conformational changes were observed in ESV1, but this can be explained by the fact that the protein has a reduced N-terminal domain and consists almost entirely of the highly structured C-terminal conserved domain, which is unlikely to undergo conformational changes.

As the experiments we carried out were with amylopectin molecules in its solubilized form, we wanted to verify that ESV1 and LESV were able to interact with the crystallized form. The results we obtained in fluorescence microscopy with maize *waxy* starch granules, which contain no amylose, showed that ESV1 and LESV interact directly with amylopectin starch granules. In fact, the two proteins, identified by their inherent fluorescence, accumulated on the entire surface of the starch granules. This result confirms those obtained in solution and is consistent with the role described in our recent work (Liu et al., 2023).

LESV is able to bind to amylopectin during its biosynthesis

In this work we further showed that the two proteins behave differently toward glycogen as only LESV was able to interact with it. This finding is very interesting on several levels. First, it shows that the difference in affinity of ESV1 for amylopectin and amylose does not seem to be related to the presence of branch points, but rather to the three-dimensional structure of the glucan. Secondly, an analogy has been drawn between the structure of

glycogen and that of the precursor molecules of amylopectin during its biosynthesis, before the action of isoamylases that remove the excess branching points (Ball et al., 1996). This result strengthens the proposed function of LESV in our previous work (Liu et al., 2023). On the one hand, LESV could function concomitantly with isoamylases during the biosynthesis of amylopectin - supporting the phase transition of double helices (from soluble to semi-crystalline form), as the branching pattern is optimized. However, on the other hand, we showed that LESV can also promote the phase transition of nascent amylopectin even if it is not debranched by isoamylase and would otherwise remain soluble as phytoglycogen (Liu et al., 2023). Our results are also consistent with the idea that ESV1 functions downstream of LESV, stabilizing newly formed starch granules. Thus, while ESV1 has an affinity for the amylopectin after the isoamylases have optimized its structure for crystallization, it has a low affinity for glycogen, which will not undergo phase transition of its own accord.

LESV and ESV1 share a common domain whose structure was modelled and described as being particularly compatible with the binding of amylopectin double helices. The fact that ESV1, which is predominantly composed of this domain, does not interact with glycogen suggests that the interaction with the nascent amylopectin is mediated or assisted by the N-terminal domain of LESV, which giving it additional specificity and allowing it to accommodate different glucans than ESV1. Indeed, we previously noted that the N-terminus of LESV also has highly conserved aromatic amino acids in parts of the protein that are predicted either to be in α-helical structure or to be unstructured (Liu et al., 2023). It will be interesting to examine the roles of these residues in future studies.

The C-terminal domain is able to bind at least two double helices of amylopectin

The models obtained for ESV1 and LESV *via* Alphafold2 provided a very reliable structure for the C-terminal tryptophan-rich domain, which is conserved between the two molecules. The other parts of the molecule were predicted without much reliability (Liu et al., 2023). The C-terminal domain folded into an original structure, forming a rather large oval (about 40 Å wide and 70Å long) antiparallel twisted ß-sheet. On this β-sheet, the aromatic and acidic residues, organized in repeated sequences identified during the analysis of the protein sequences, form parallel lines equidistant from each other and parallel to the axis of the β-sheet. The side chains of these amino acids point alternately to both sides of the ß-sheet. However, one face of the β-sheet may be “occupied” by a long α-helix in LESV and a long loop in ESV1. Therefore, we computed models where only the “free” side interacted with

amylopectin double helices. Even though we observed protein conformational changes in the presence of amylopectin, based on our current data, we do not know if the protein parts on the occupied face can move to expose the lines of aromatic and acidic residue for additional amylopectin binding. If that does occur, ESV1 and LESV could bind amylopectin on both sides of their β-sheet, resulting in sandwich-like alignments of proteins and amylopectin.

We were able to demonstrate experimentally that LESV and ESV1 can bind amylopectin in both its soluble form and its organized form within starch granules. Furthermore, our modelling work shows that this interaction likely occurs through the shared β-sheet domain via both the aromatic and acidic residues. Moreover, we suggested that the unique structure of this domain enables it to bind at least two parallel double helices of amylopectin in a parallel arrangement similar to that found in the crystalline regions of starch granules, thereby supporting its proposed function in the organization and maintenance of starch granules in plants.

The N-terminal domain allows regulation of LESV specificity towards starch components.

The structure of the N-terminal domain of LESV is not known. However, we have been able to demonstrate that it consists mainly of disordered regions and α-helices that may be organized close to the C-terminal domain. We have also shown that interaction with amylopectin induces the formation of α-helices presumably from the disordered regions without affecting the β-sheet structure. In ESV1, this domain N-terminal domain is shorter, and poorly conserved between species, but still predicted to be unstructured, as is the polyproline tail at the C-terminus of the Arabidopsis protein. It is likely that the presence of these regions prevented us from obtaining protein crystals. Since amylopectin structure and size is not monodisperse, it cannot be used to stabilize the proteins, and we are currently searching for analogues that can facilitate the crystallization of both proteins. While analyzing the structure of the C-terminal domains has allowed us to describe the interaction mode of the two proteins with amylopectin, analyzing the entire structures, particularly for LESV, would help us to elucidate the function of the N-terminal domain, potentially revealing the mechanism of LESV action in promoting amylopectin crystallization, and explaining the difference between it and ESV1. Considering that several helices are present in the LESV N-terminus, and taking into account its involvement in amylopectin biosynthesis, it

is possible that LESV may also interact with other proteins, as already described for SSs and BEs (Ahmed et al., 2015; Crofts et al., 2015).

In conclusion, this work improves our understanding of the molecular mechanisms of ESV1 and LESV function in Arabidopsis. We have shown that the conserved C-terminal domain of both ESV1 and LESV is particularly well suited to bind amylopectin double helices as they are organized in starch granules. We further propose that LESV is able to interact with nascent amylopectin molecules during its biosynthesis, and that its involvement in the phase transition probably occurs before the biosynthesis process is complete. Our data are consistent with the idea that ESV1 would intervene later to stabilize the granules to prevent early degradation by hydrolytic activities. Further research is needed to describe the precise molecular mechanism of ESV1 and LESV function in plants. Resolution of the atomic structures of the entire LESV, particularly the organization of its N-terminal domain in relation to its glucan binding domain and its interaction with starch glucans will allow considerable progress to be made in this area. Finally, studying the function of these proteins in other plants - specifically their involvement in storage starch biosynthesis - will be important to assess their candidacy as targets for starch crop improvement through biotechnological approaches.

Materials and Methods

Cloning, expression, and purification of proteins

LESV and ESV1 from Arabidopsis (*Arabidopsis thaliana*) were cloned, expressed in *Escherichia coli* as recombinant proteins lacking their N-terminal transit peptides, and purified as described previously. The purification batches of proteins used in this work are the same than those used in previous work (see Figure S2 in (Liu et al., 2023)). Purification was performed by a first step of Immobilized Metal Affinity Chromatography followed by a second purification step through size exclusion chromatography using a HiLoad 16/60 Superdex 200 (Cytiva) column pre-equilibrated with 50 mM Tris-HCl, pH 8, 150 mM NaCl, 10% (w/v) glycerol, 2 mM DTT for LESV or a dialysis step against 50 mM Tris-HCl, pH 7.5, 100 mM NaCl, 10% (v/v) glycerol, 2 mM DTT for ESV1. The monodispersity of the obtained protein solution was assessed by dynamic light scattering (DLS) using a zetasizer pro (Malvern Panalytical). For structural study, protein samples were concentrated using

Vivaspin centrifugal concentrator with a 10 kDa cut-off (Sartorius). Protein concentrations were determined using a Nanodrop Spectrophotometer (ND1000) from Thermo Scientific.

Glucan solution preparation

For EMSA experiments, amylose 1% (w/v), amylopectin 1% (w/v) and glycogen 5% (w/v) stock solutions used for these experiments were prepared as follows. 0.1 g of amylose [from potato (*Solanum tuberosum*); Sigma] was dissolved in 1 ml of 2 M sodium hydroxide (NaOH) and vortexed to ensure complete solubilization. After addition of 2 ml of deionized water, the solution was neutralized by 1 ml of 2 M HCl. The final volume was then adjusted to 10 ml with water and the solution was heated 5 min at 50°C and vortexed until complete dissolution. Amylopectin (0.1 g, from potato, Sigma) was resuspended in 10 ml of distilled water and then subjected to autoclaving to produce a homogeneous solution. Glycogen powder [0.5 g, from oyster (*Ostrea edulis*); Sigma] was dissolved by vortexing it in distilled water (final volume 10 ml) until full homogenization. For CD experiments, glucan stock solutions were prepared with the same protocol albeit replacing water with protein buffer.

Electromobility Shift Assays (EMSAs)

One microgram of ESV1, LESV, and a reference protein with no affinity for glucans (Uniprot Q7W019 produced in the lab (Herrou et al., 2007)) were loaded on 8% (w/v) polyacrylamide gels containing increasing concentrations of glucans (from 0.1 to 0.3% [w/v] for amylopectin and amylose, and 0.1 to 1% [w/v] for glycogen) and submitted to electrophoresis in native conditions at 4°C at 15 V cm^{-1} for 2 h in 25 mM Tris-HCL, pH 8.3, 192 mM glycine migration buffer. Gels were stained with InstantBlue^{TM} (Expedeon). The affinity of LESV and ESV1 for the different glucans in the gels was estimated by the migration shift of these proteins compared to the stable migration of the reference protein, either loaded alone or mixed with ESV1 or LESV.

Synchrotron radiation circular dichroism

Synchrotron radiation circular dichroism (SR-CD) spectra were measured at the DISCO beamline of the SOLEIL Synchrotron (Gif-sur-Yvette, France). Five microliters of ESV1 protein at 6.1 mg ml^{-1} and 2 µl of LESV protein at 13.4 mg ml^{-1} were deposited between 2 CaF_2 coverslips with a pathlength of 20 µm and 10 µm respectively (Refregiers et al., 2012).

The beam size of 4 × 4 mm and the photon-flux per nm step of 2×10^{10} photons s^{-1} in the spectral band from 270–170 nm prevented radiation-induced damage (Miles et al., 2008). CD spectra were acquired using IGOR software (WaveMetrics). Protein and buffer spectra were collected consecutively and are the mean of 3 accumulations. The buffer baseline was recorded sequentially and subtracted from the spectra before taking into account the protein concentration. Before measurements the molar elliptical extinction coefficient of Ammonium *d*-10-Camphorsulfonate Ammonium (CSA) has been measured on the beamline and used as standard for calibration of all data measurements (Miles et al., 2004). Data processing was conducted using CDToolX software (Miles and Wallace, 2018). The influence of the different glucans on the structure of LESV and ESV1 was studied by incubating the protein/glucan mixtures for 2 h and measuring the spectra under the same conditions as for the native proteins. The mixtures were made with 4:1 mix of protein solution and glucan solution (1% [w/v] amylose or amylopectin solutions). Five microliters of ESV1/glucans mixtures and 2 µl of LESV/glucan mixtures were deposited between 2 CaF_2 coverslips with a pathlength of 20 µm and 10 µm respectively (Refregiers et al., 2012). Spectra containing 80% v/v of protein buffer and 20% glucan solutions were subtracted from the protein/glucan spectra before CSA calibration. Temperature scans were realized to check the protein stabilization by glucan interaction. CD spectra were collected from 20-30°C to 90°C and processed as described above with 3-5°C temperature increases and 3 min of equilibration time. The secondary structure element content of each protein alone or in the presence of glucans was estimated using BestSel (Micsonai et al., 2015).

Molecular Modelling

Protein structures of LESV and ESV1 were modelled using AlphaFold2 (Jumper et al., 2021). For each protein, five different models were computed and ranked by global predicted Local Distance Difference Test (pLDDT). The five molecular models generated were superimposed and used to evaluate the possible position of dynamic regions. Molecular models with best pLDDT values were used for figures and further molecular docking studies.

Small-Angle-X-ray-Scattering (SAXS)

Protein sample solutions were centrifuged for 10 min at 10,000 g prior to X-ray analysis as a precaution to remove any insoluble aggregates. SAXS experiments were conducted on the SWING beamline at Synchrotron SOLEIL (λ= 1.033 Å). All solutions were mixed in a fixed-

582 temperature (15°C) quartz capillary. The monodisperse sample solutions of proteins were
583 injected onto a size exclusion column (David and Perez, 2009) (SEC-3, 150 Å; Agilent) using
584 an Agilent HPLC system and eluted into the capillary cell at a flow rate of 0.3 ml min^{-1}.
585 Then, 50 µl of protein samples were injected for SAXS measurements. 180 frames were
586 collected during the first minutes of the elution and were averaged to account for buffer
587 scattering and subtracted from selected frames corresponding to the main protein elution
588 peak. Data reduction to absolute units, frame averaging, and subtraction were done using
589 FOXTROT (David and Perez, 2009). Data processing, analysis, and modeling steps were
590 carried out using programs of the ATSAS suite (Franke et al., 2017). BUNCH (Petoukhov
591 and Svergun, 2005) was used to model the missing parts of the proteins that were not
592 assigned by Alphafold2 (Jumper et al., 2021). The fit of the model obtained with BUNCH to
593 the experimental SAXS data is estimated by superimposing the SAXS curve derived from the
594 model on the measured SAXS curve. A low χ^2 value indicates a good superposition of the
595 curves and therefore that the model is compatible with the experimental data.

596 **Docking**

597 Alphafold2 model structures of the conserved C-terminal domain of ESV1 and LESV were
598 used as targets in order to model the binding position of the model of a double helix of
599 amylopectin obtained from Polysac3DB (CERMAV https://polysac3db.cermav.cnrs.fr). A
600 generic algorithm was used for the search step within a sphere of 10 Å centred on the
601 tryptophan stripes of the conserved β-sheet domain. The scoring function was based on the
602 ChemPLP forcefield, as used by GOLD (Jones et al., 1997). All the parameters were kept by
603 default. A subsequent energy minimization was performed on the best model using the
604 Amber forcefield. All figures representing molecular structures of proteins and ligands were
605 generated using Pymol (The PyMOL Molecular Graphics System, version 1.8.0.0
606 Schrödinger, LLC).

607 **3-D imaging**

608 For this experiment we used *waxy* maize starch granules (Roquette, France) obtained from
609 plants lacking granule-bound starch synthase (GBSS;(Tsai, 1974)), the enzyme that catalyzes
610 the biosynthesis of amylose and whose presence in the granules is responsible of their
611 autofluorescence. Starch granules were washed with water, acetone and ethanol in order to
612 remove any phenol contaminants coming from storage in plasticware (Tawil et al., 2011).

ESV1 and LESV binding on starch granules was assessed by both visible and UV microscopy with the same protocol described in (Jamme et al., 2014). Excitation was set-up at λ=280 nm with an emission filter at 329-351 nm (FF01-340/22, Semorock) to visualize the tryptophan emission (at 345 nm) of bound proteins. The acquisition time was 10 s for each emission fluorescence image and 0.2 s for visible images. For 3D purpose, Z slices (along the optical axis) were recorded with a step size of 300 nm over 40 µm Z range under µManager control (Edelstein et al., 2010). Using imaging analysis software (Huygens, SVI, NL), deconvolution images were calculated by PSF deconvolution treatment. Images were coupled to classical light imaging of the starch granule morphology. Images were analyzed using FiJi (Schindelin et al., 2012). Noise was removed from acquired 3-D stacks using a median 1 filter. A substack of "in focus" images were selected and summed. To compensate for field inhomogeneity, a FFT bandbass filter was then applied.

Accession Numbers

The Arabidopsis Genome Initiative gene codes for the Arabidopsis genes used in this study are as follows: *ESV1, At1g42430; LESV, At3g55760*.

Funding information

This work has been supported by CNRS (core funding to CS, DD, CB and PhD grant for RO), Université de Lille (core funding to CdH and PhD grant to MB) and Région Hauts de France (PhD grant for MB)

Acknowledgments

The authors strongly acknowledge DISCO beamline and the regular access to the small angle X-ray scattering beamline SWING at synchrotron SOLEIL (St Aubin, France) through the BAG MX-20181002 and MX-20201190, and are grateful for the expert technical support provided by beamline staffs.

Author Contributions

CB and RO conceived and designed the experiment with input from SZ, DD and CdH. RO and CB performed experiments with input from MB, CL and CS. CB, RO and MB collected synchrotron data. CB and RO analyzed data with the input of MB and DD. CB wrote the manuscript. CB, DD, CdH, SZ and CS revised the manuscript.

Figure Legends

Figure 1: Structure of LESV of *Arabidopsis thaliana*. The structure is represented in cartoon. **A)** Superposition of the 5 molecular models of LESV calculated with Alphafold 2. Only regions with pLDDT > 70 are shown except for the first model (light gray). Regions common to all 5 models with pLDDT > 90 are colored dark grey. The helices of the 5 models are colored in light grey, salmon, cyan, yellow and green. The common helix with ESV1 is on the left, the long helix specific for LESV is on the right. B) *ab initio* model of the N-terminal domain of LESV computed from SAXS data using the software BUNCH. The conserved C-terminal domain is represented as cartoon and colored in dark blue, the N-terminal domain model is represented as spheres (one sphere by amino acid residue) and colored in green C) Superposition of SAXS experimental data obtained for LESV (cyan) and calculated curve from BUNCH model (black) with χ^2= 3.8Å.

Figure 2: Structure of C-terminal domains of LESV and ESV1. A) Conserved structural motifs on Face A of LESV and B) ESV1 . The structures are represented as cartoon, the common β-sheet is colored in magenta, the common C-terminal helix is colored in cyan and the long helix of LESV (A) and the long loop of ESV1 (B) are colored in yellow. The right panel is another view of the left panel after a rotation of 90° along the y-axis.

Figure 3: EMSA gels analyzing the interaction between ESV1 or LESV and starch glucans. A) interaction with amylopectin B) interaction with amylose and C) interaction with glycogen. Blue, red and yellow arrows indicate the bands corresponding to the reference protein, ESV1 and LESV respectively. The migration shift is indicated by a black arrow.

Figure 4: SR-CD spectra for ESV1 alone (grey), and in presence of amylopectin (red) or amylose (blue). The composition in secondary structural elements evaluated by BestSel are in inset. NRMSD is the normalized root mean square deviation

Figure 5: SR-CD spectra for LESV alone (grey), and in presence of amylopectin (red) or amylose (blue). The composition in secondary structural elements evaluated by BestSel are in inset. NRMSD is the normalized root mean square deviation.

Figure 6: Thermal denaturation of LESV and ESV1 followed by the variation of the SR-CD molar ellipticity in function of the temperature. Plots represent consecutive scans on the protein collected at a set of temperature between 20 to 90°C colored in a gradient from dark

blue (lowest temperature) to light blue (highest temperature) for A) LESV alone, B) LESV with amylopectin C) ESV1 alone, D) ESV1 with amylopectin. From these spectra molar ellipticity at wavelength indicated by an arrow on the scans, molar ellipticity in function of the temperature have been used to monitor E) thermal denaturation of LESV followed at λ=195nm F) thermal denaturation of ESV1followed at λ=190nm. Curves corresponding to proteins alone or combined with amylopectin are colored in grey and red respectively

Figure 7: Transmitted light and fluorescence imaging of maize waxy starch granules in the presence of ESV1 (top panel), LESV (medium panel) and BSA (low panel) as negative control. A) visible light imaging B) fluorescence images of ESV1 or LESV absorption on starch granules C) combination of visible light and fluorescence images. (scalebar for all images: 50µm)

Figure 8: Molecular model of the complex between C-terminal domain of LESV and amylopectin double helices. Protein chain is represented in cartoon and colored in blue. Aromatic residues are colored in magenta and their side chains are represented by sticks. Amylopectin double helices are represented by sticks and colored by atom types.

References

Ahmed Z, Tetlow IJ, Ahmed R, Morell MK, Emes MJ (2015) Protein-protein interactions among enzymes of starch biosynthesis in high-amylose barley genotypes reveal differential roles of heteromeric enzyme complexes in the synthesis of A and B granules. Plant Sci **233:** 95-106

Ball S, Guan HP, James M, Myers A, Keeling P, Mouille G, Buleon A, Colonna P, Preiss J (1996) From glycogen to amylopectin: a model for the biogenesis of the plant starch granule. Cell **86:** 349-352

Buleon A, Colonna P, Planchot V, Ball S (1998) Starch granules: structure and biosynthesis. Int J Biol Macromol **23:** 85-112

Crofts N, Abe N, Oitome NF, Matsushima R, Hayashi M, Tetlow IJ, Emes MJ, Nakamura Y, Fujita N (2015) Amylopectin biosynthetic enzymes from developing rice seed form enzymatically active protein complexes. J Exp Bot **66:** 4469-4482

David G, Perez J (2009) Combined sampler robot and high-performance liquid chromatography: a fully automated system for biological small-angle X-ray scattering experiments at the Synchrotron SOLEIL SWING beamline. Journal of applied crystallography **42:** 9

Delatte T, Trevisan M, Parker ML, Zeeman SC (2005) Arabidopsis mutants Atisa1 and Atisa2 have identical phenotypes and lack the same multimeric isoamylase, which influences the branch point distribution of amylopectin during starch synthesis. Plant J **41:** 815-830

Edelstein A, Amodaj N, Hoover K, Vale R, Stuurman N (2010) Computer control of microscopes using microManager. Curr Protoc Mol Biol **Chapter 14:** Unit14 20

Feike D, Seung D, Graf A, Bischof S, Ellick T, Coiro M, Soyk S, Eicke S, Mettler-Altmann T, Lu KJ, Trick M, Zeeman SC, Smith AM (2016) The Starch Granule-Associated Protein EARLY STARVATION1 Is Required for the Control of Starch Degradation in Arabidopsis thaliana Leaves. Plant Cell **28:** 1472-1489

Franke D, Petoukov MV, Konarev PV, Panijkovich A, Tuukkanen A, Mertens HDT, Kikhney NR, Hajizadeh NR, Franklin JM, Jeffries CM, Svergun D (2017) ATSAS 2.8: a comprehensive data analysis suite for small-angle scattering from macromolecular solutions. Journal of applied crystallography **50:** 1212-1225

Helle S, Bray F, Verbeke J, Devassine S, Courseaux A, Facon M, Tokarski C, Rolando C, Szydlowski N (2018) Proteome Analysis of Potato Starch Reveals the Presence of New Starch Metabolic Proteins as Well as Multiple Protease Inhibitors. Front Plant Sci **9:** 746

Herrou J, Bompard C, Antoine R, Leroy A, Rucktooa P, Hot D, Huvent I, Locht C, Villeret V, Jacob-Dubuisson F (2007) Structure-based mechanism of ligand binding for periplasmic solute-binding protein of the Bug family. J Mol Biol **373:** 954-964

Hussain R, Javorti T, Siligardi G, eds (2012) Spectroscopic analysis: synchrotron radiation circular dichroism., Vol 8. Elsevier, Amsterdam

Hussain R, Longo E, Siligardi G (2018) UV-denaturation assay to assess protein photostability and ligand-binding interactions using the high photon flux of diamond B23 beamline for SRCD. . Molecules **23**

Imberty A, Chanzy H, Perez S, Buleon A, Tran V (1988) The double-helical nature of the crystalline part of A-starch. J Mol Biol **201:** 365-378

Jamme F, Bourquin D, Tawil G, Vikso-Nielsen A, Buleon A, Refregiers M (2014) 3D imaging of enzymes working in situ. Anal Chem **86:** 5265-5270

Jones G, Willett P, Glen RC, Leach AR, Taylor R (1997) Development and validation of a genetic algorithm for flexible docking. J Mol Biol **267:** 727-748

Jumper J, Evans R, Pritzel A, Green T, Figurnov M, Ronneberger O, Tunyasuvunakool K, Bates R, Zidek A, Potapenko A, Bridgland A, Meyer C, Kohl SAA, Ballard AJ, Cowie A, Romera-Paredes B, Nikolov S, Jain R, Adler J, Back T, Petersen S, Reiman D, Clancy E, Zielinski M, Steinegger

M, Pacholska M, Berghammer T, Bodenstein S, Silver D, Vinyals O, Senior AW, Kavukcuoglu K, Kohli P, Hassabis D (2021) Highly accurate protein structure prediction with AlphaFold. Nature **596:** 583-589

Larson ME, Falconer DJ, Myers AM, Barb AW (2016) Direct Characterization of the Maize Starch Synthase IIa Product Shows Maltodextrin Elongation Occurs at the Non-reducing End. J Biol Chem **291:** 24951-24960

Liu C, Pfister B, Osman R, Ritter M, Heutinck A, Sharma M, Eicke S, Fischer-Stettler M, Seung D, Bompard C, Abt MR, Zeeman SC (2023) LIKE EARLY STARVATION 1 and EARLY STARVATION 1 promote and stabilize amylopectin phase transition in starch biosynthesis. Sci Adv **9:** eadg7448

Liu C, Pfister B, Osman R, Ritter M, Heutinck A, Sharma M, Eicke S, Fisher-Stettler M, Seung D, Bompard C, Abt MR, Zeeman SC (2023) LIKE EARLY STARVATION 1 and EARLY STARVATION 1 Promote and Stabilize Amylopectin Phase Transition in Starch Biosynthesis. Science Advances **In press**

Malinova I, Mahto H, Brandt F, Al-Rawi S, Qasim H, Brust H, Hejazi M, Fettke J (2018) EARLY STARVATION1 specifically affects the phosphorylation action of starch-related dikinases. Plant J **95:** 126-137

Micsonai A, Wien F, Kernya L, Lee YH, Goto Y, Refregiers M, Kardos J (2015) Accurate secondary structure prediction and fold recognition for circular dichroism spectroscopy. Proc Natl Acad Sci U S A **112:** E3095-3103

Miles AJ, Janes RW, Brown A, Clarke DT, Sutherland JC, Tao Y, Wallace BA, Hoffmann SV (2008) Light flux density threshold at which protein denaturation is induced by synchrotron radiation circular dichroism beamlines. J Synchrotron Radiat **15:** 420-422

Miles AJ, Wallace BA (2018) CDtoolX, a downloadable software package for processing and analyses of circular dichroism spectroscopic data. Protein Sci **27:** 1717-1722

Miles AJ, Wien F, Wallace BA (2004) Redetermination of the extinction coefficient of camphor-10-sulfonic acid, a calibration standard for circular dichroism spectroscopy. Anal Biochem **335:** 338-339

Myers AM, Morell MK, James MG, Ball SG (2000) Recent progress toward understanding biosynthesis of the amylopectin crystal. Plant Physiol **122:** 989-997

Pérez S, Bertoft E (2010) The molecular structures of starch components and their contribution to the architecture of starch granules: A comprehensive review. . Starch-Stärke **62:** 389-420

Petoukhov MV, Svergun DI (2005) Global rigid body modeling of macromolecular complexes against small-angle scattering data. Biophys J **89:** 1237-1250

Pfister B, Lu KJ, Eicke S, Feil R, Lunn JE, Streb S, Zeeman SC (2014) Genetic Evidence That Chain Length and Branch Point Distributions Are Linked Determinants of Starch Granule Formation in Arabidopsis. Plant Physiol **165:** 1457-1474

Pfister B, Zeeman SC (2016) Formation of starch in plant cells. Cell Mol Life Sci **73:** 2781-2807

Refregiers M, Wien F, Ta HP, Premvardhan L, Bac S, Jamme F, Rouam V, Lagarde B, Polack F, Giorgetta JL, Ricaud JP, Bordessoule M, Giuliani A (2012) DISCO synchrotron-radiation circular-dichroism endstation at SOLEIL. J Synchrotron Radiat **19:** 831-835

Sawada T, Nakamura Y, Ohdan T, Saitoh A, Francisco PB, Jr., Suzuki E, Fujita N, Shimonaga T, Fujiwara S, Tsuzuki M, Colleoni C, Ball S (2014) Diversity of reaction characteristics of glucan branching enzymes and the fine structure of alpha-glucan from various sources. Arch Biochem Biophys **562:** 9-21

Schindelin J, Arganda-Carreras I, Frise E, Kaynig V, Longair M, Pietzsch T, Preibisch S, Rueden C, Saalfeld S, Schmid B, Tinevez JY, White DJ, Hartenstein V, Eliceiri K, Tomancak P, Cardona A (2012) Fiji: an open-source platform for biological-image analysis. Nat Methods **9:** 676-682

Singh A, Compart J, Al-Rawi SA, Mahto H, Ahmad AM, Fettke J (2022) LIKE EARLY STARVATION 1 alters the glucan structures at the starch granule surface and thereby influences the action of both starch-synthesizing and starch-degrading enzymes. Plant J **111:** 819-835

Streb S, Delatte T, Umhang M, Eicke S, Schorderet M, Reinhardt D, Zeeman SC (2008) Starch granule biosynthesis in Arabidopsis is abolished by removal of all debranching enzymes but restored by the subsequent removal of an endoamylase. Plant Cell **20:** 3448-3466

Tawil G, Jamme F, Refregiers M, Vikso-Nielsen A, Colonna P, Buleon A (2011) In situ tracking of enzymatic breakdown of starch granules by synchrotron UV fluorescence microscopy. Anal Chem **83:** 989-993

Tsai CY (1974) The function of the waxy locus in starch synthesis in maize endosperm. Biochem Genet **11:** 83-96

Waight TA, Kato LK, Donald AM, Gidley MJ, Clarke CJ, Riekel C (2000) Side-Chain Liquid-Crystalline Model for Starch. Starch-Stärke **52:** 450-460

Wattebled F, Dong Y, Dumez S, Delvalle D, Planchot V, Berbezy P, Vyas D, Colonna P, Chatterjee M, Ball S, D'Hulst C (2005) Mutants of Arabidopsis lacking a chloroplastic isoamylase accumulate phytoglycogen and an abnormal form of amylopectin. Plant Physiol **138:** 184-195

Xie Y, Barb AW, Hennen-Bierwagen TA, Myers AM (2018) Direct Determination of the Site of Addition of Glucosyl Units to Maltooligosaccharide Acceptors Catalyzed by Maize Starch Synthase I. Front Plant Sci **9:** 1252

824 **Zeeman SC, Umemoto T, Lue WL, Au-Yeung P, Martin C, Smith AM, Chen J**
825 (1998) A mutant of Arabidopsis lacking a chloroplastic isoamylase
826 accumulates both starch and phytoglycogen. Plant Cell **10:** 1699-1712

827 **Ziegler GR, Creek JA, Runt J** (2005) Spherulitic crystallization in starch as a model
828 for starch granule initiation. Biomacromolecules **6:** 1547-1554

829

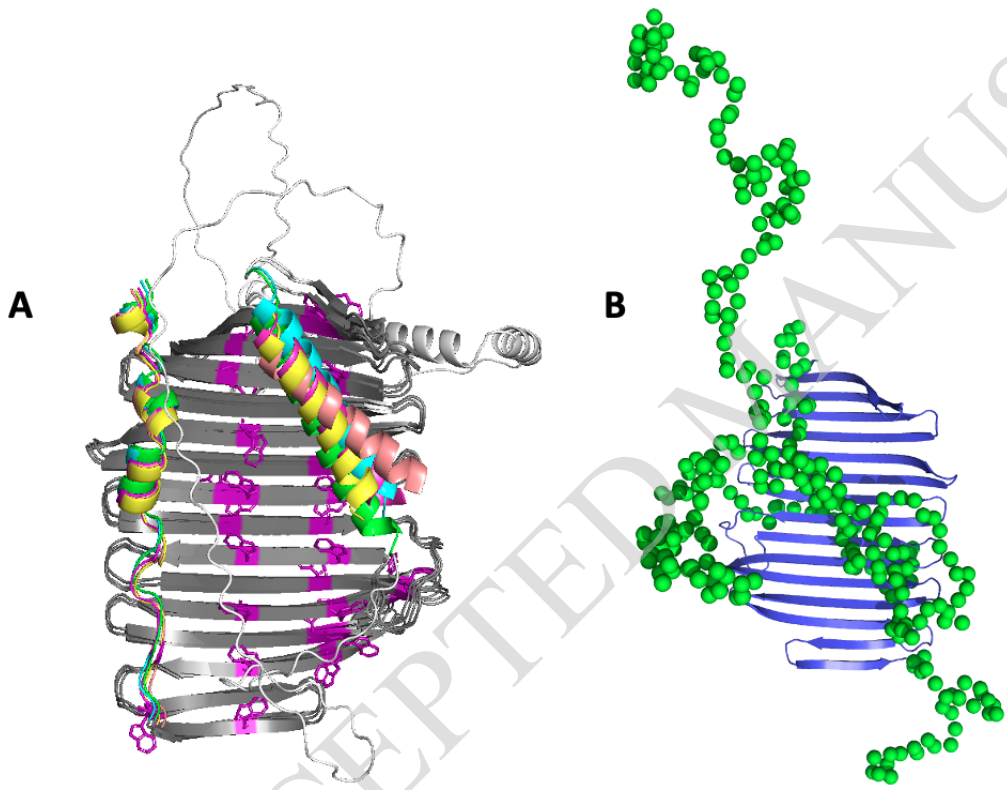

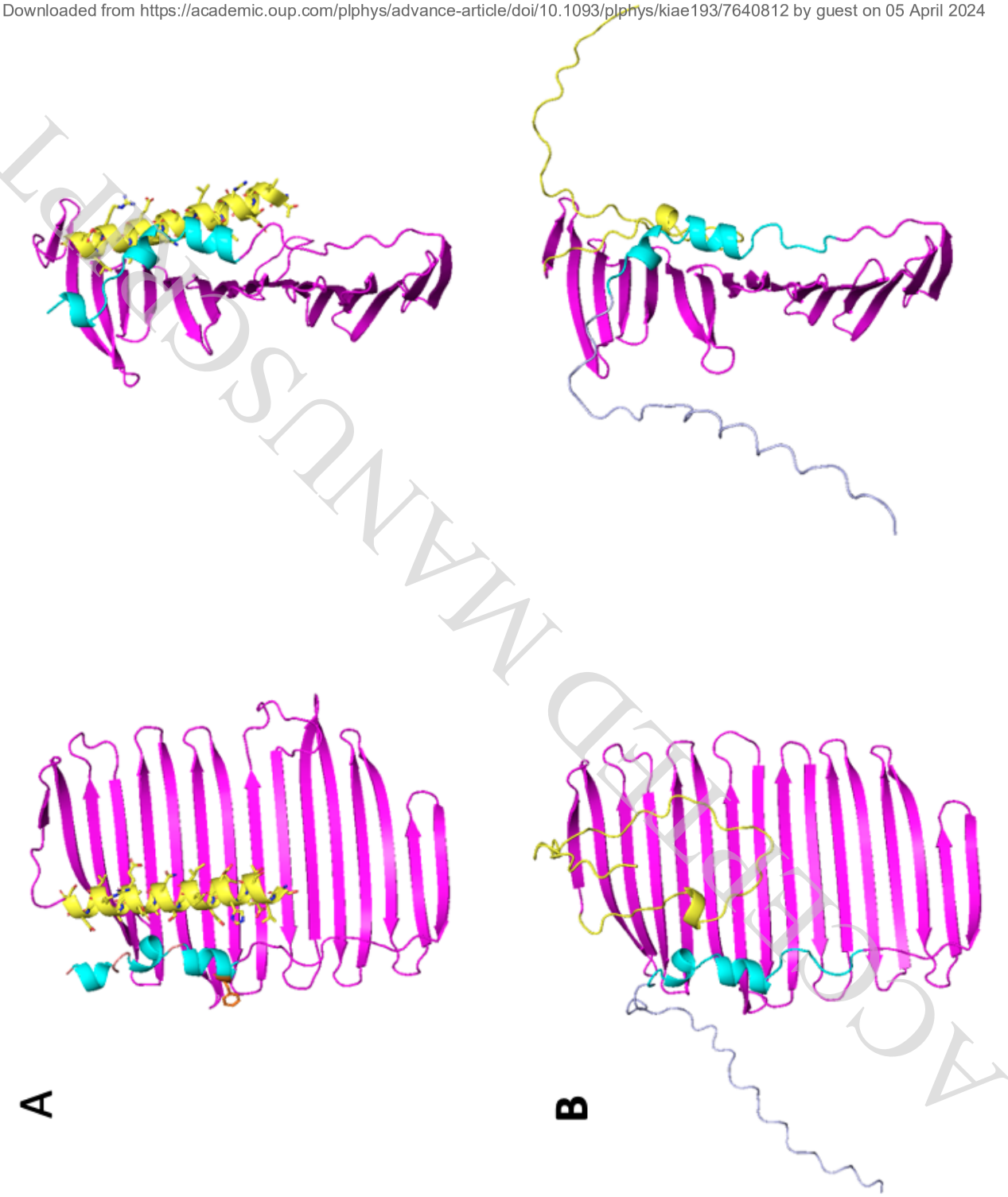

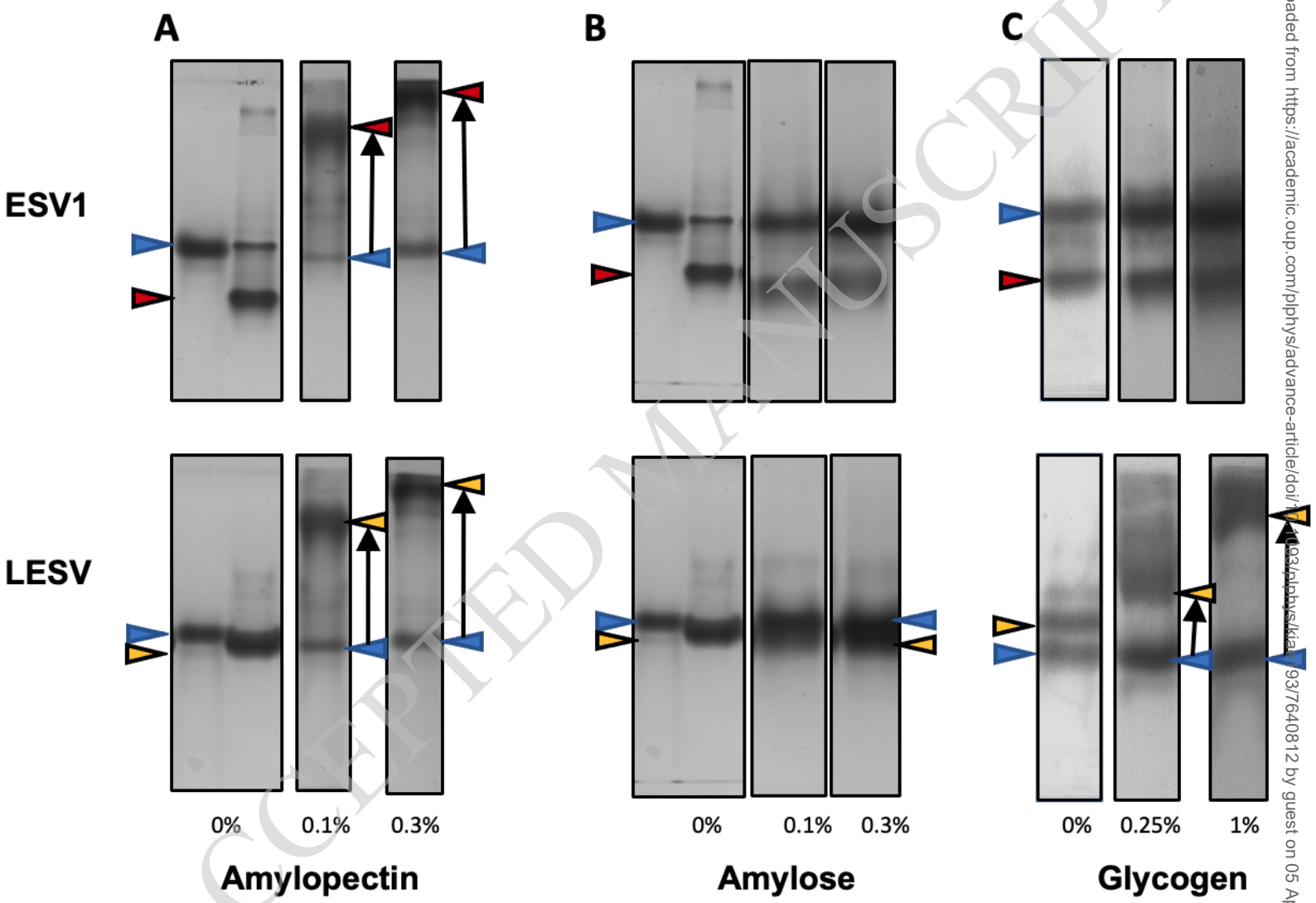

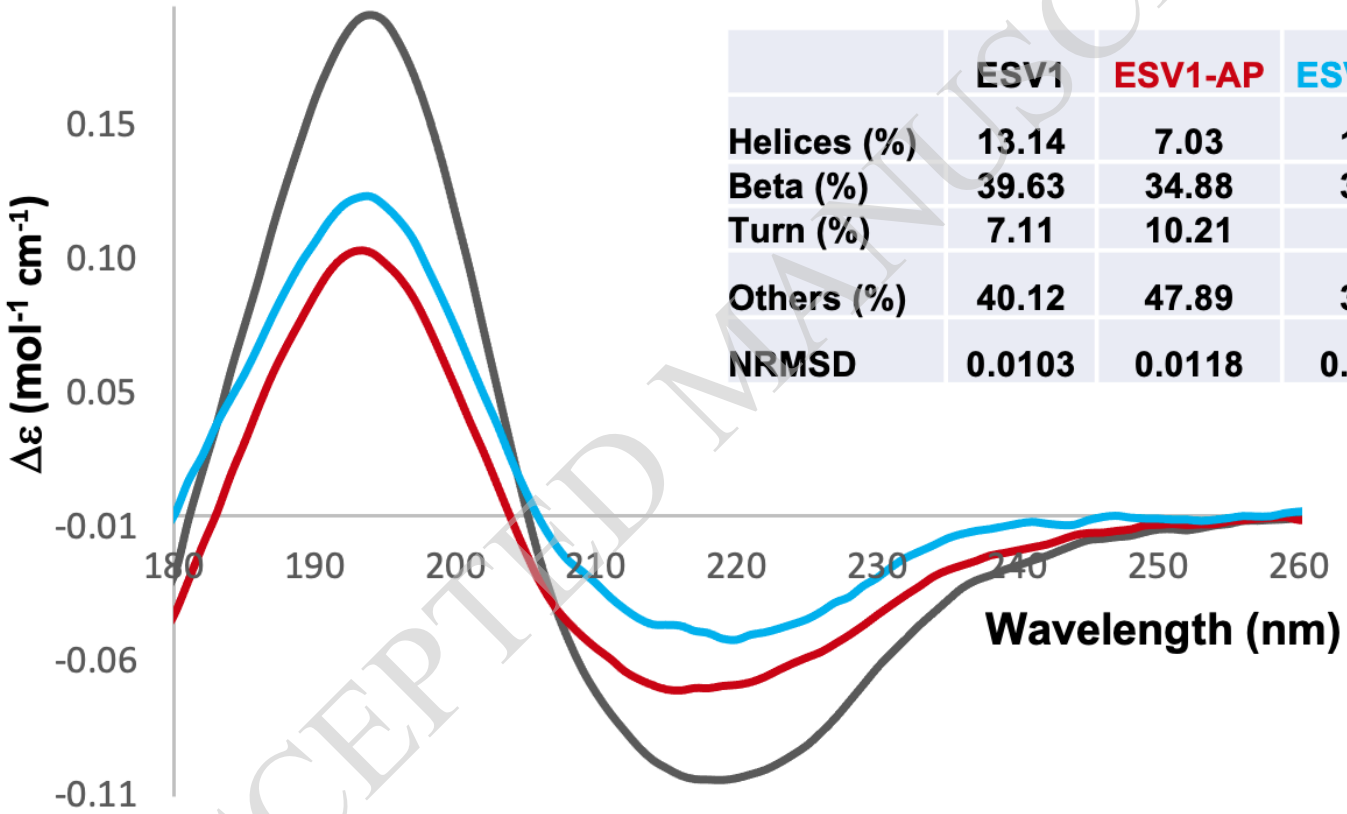

	ESV1	ESV1-AP	ESV1-AM
Helices (%)	13.14	7.03	15.7
Beta (%)	39.63	34.88	39.5
Turn (%)	7.11	10.21	7.8
Others (%)	40.12	47.89	37.1
NRMSD	0.0103	0.0118	0.0091

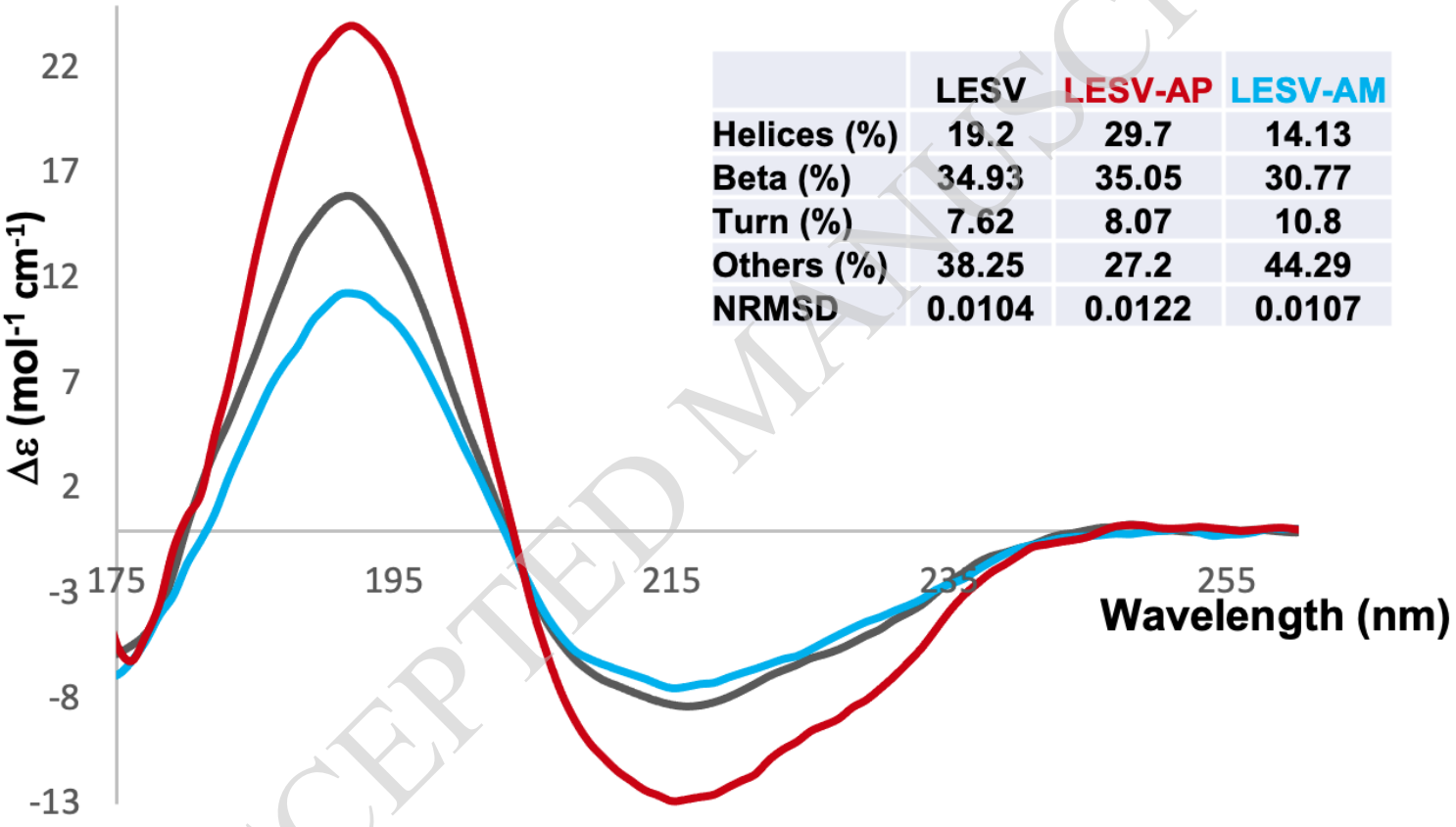

	LESV	LESV-AP	LESV-AM
Helices (%)	19.2	29.7	14.13
Beta (%)	34.93	35.05	30.77
Turn (%)	7.62	8.07	10.8
Others (%)	38.25	27.2	44.29
NRMSD	0.0104	0.0122	0.0107

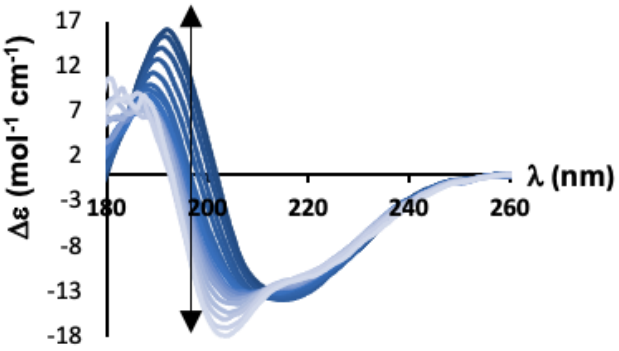

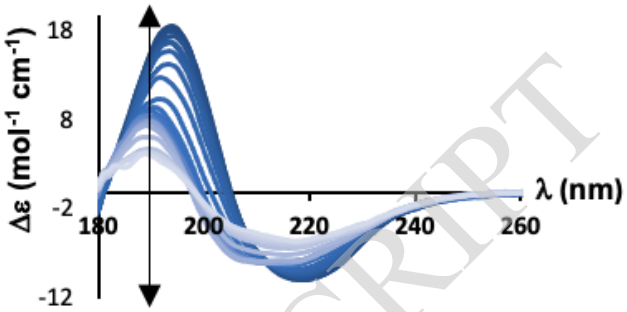

B

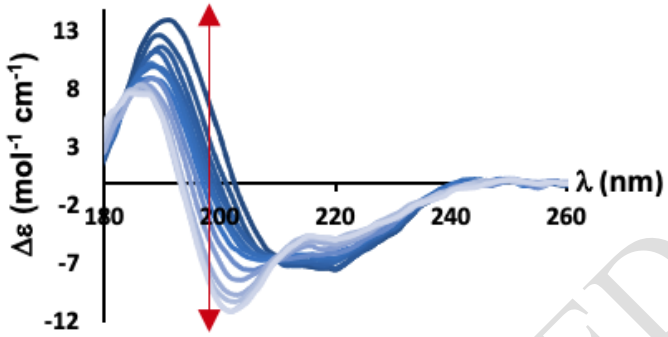

D

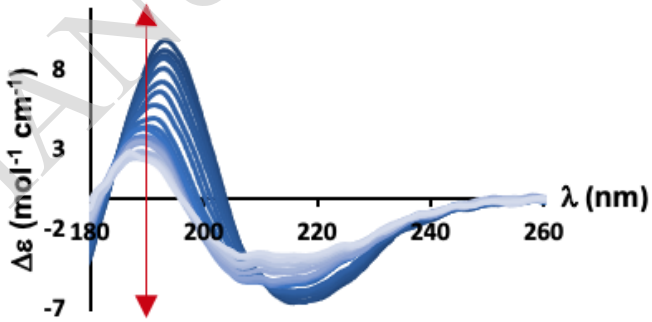

E

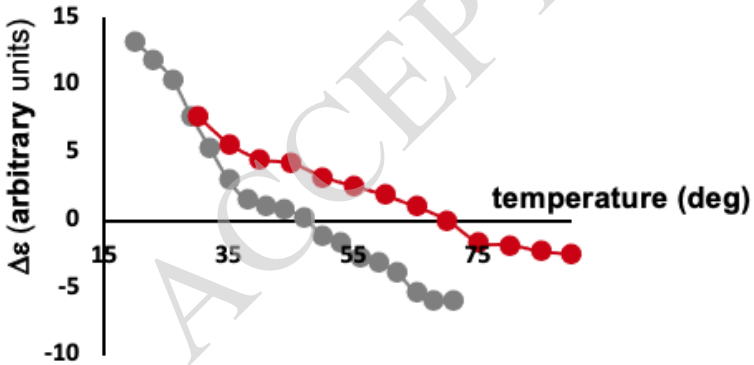

F

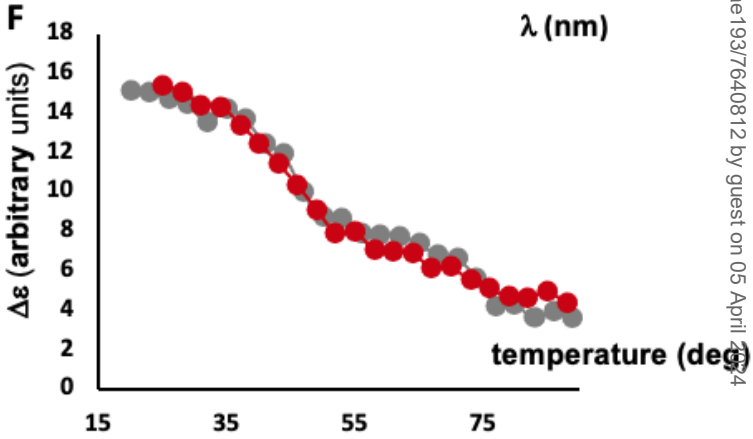

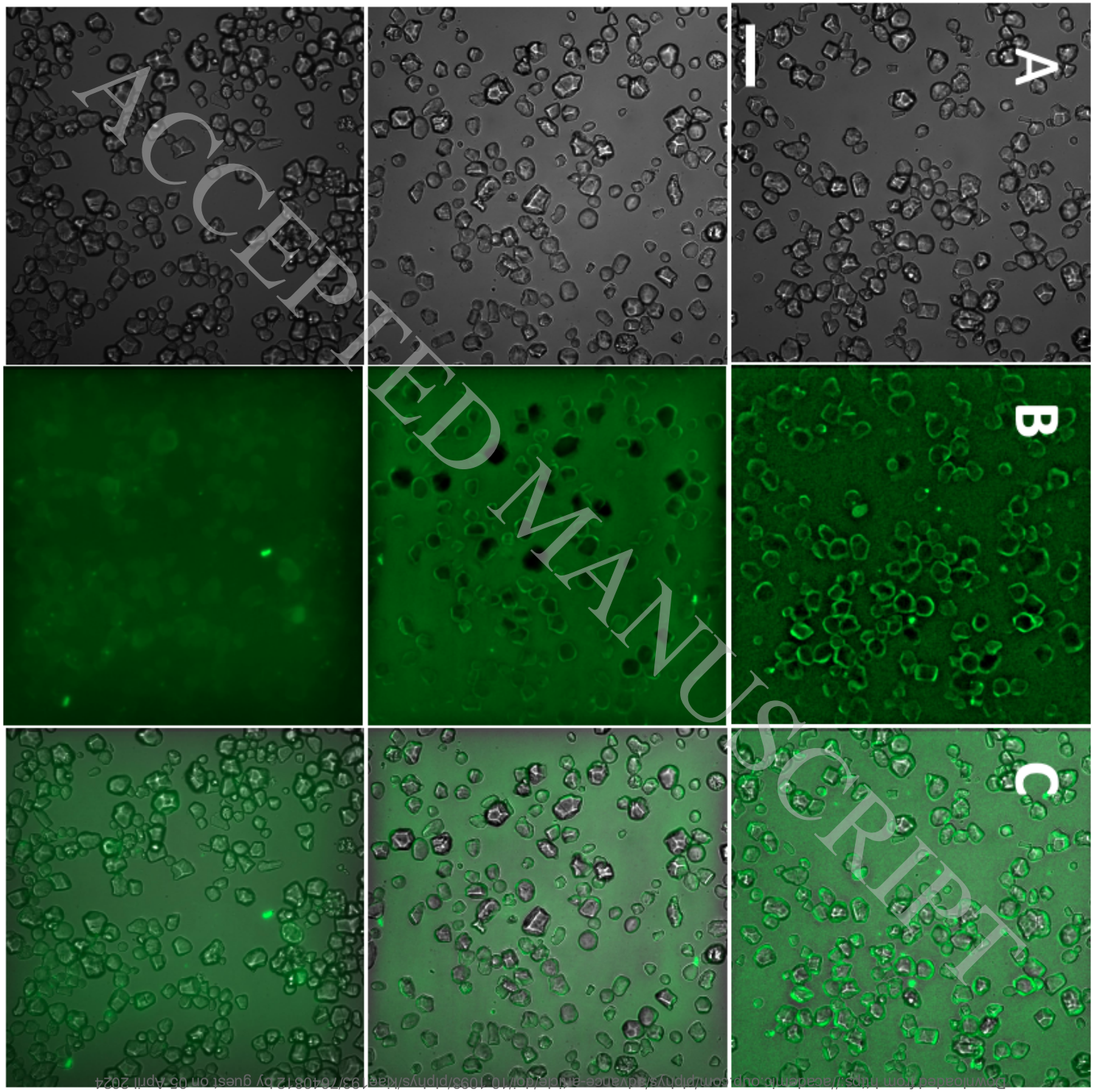

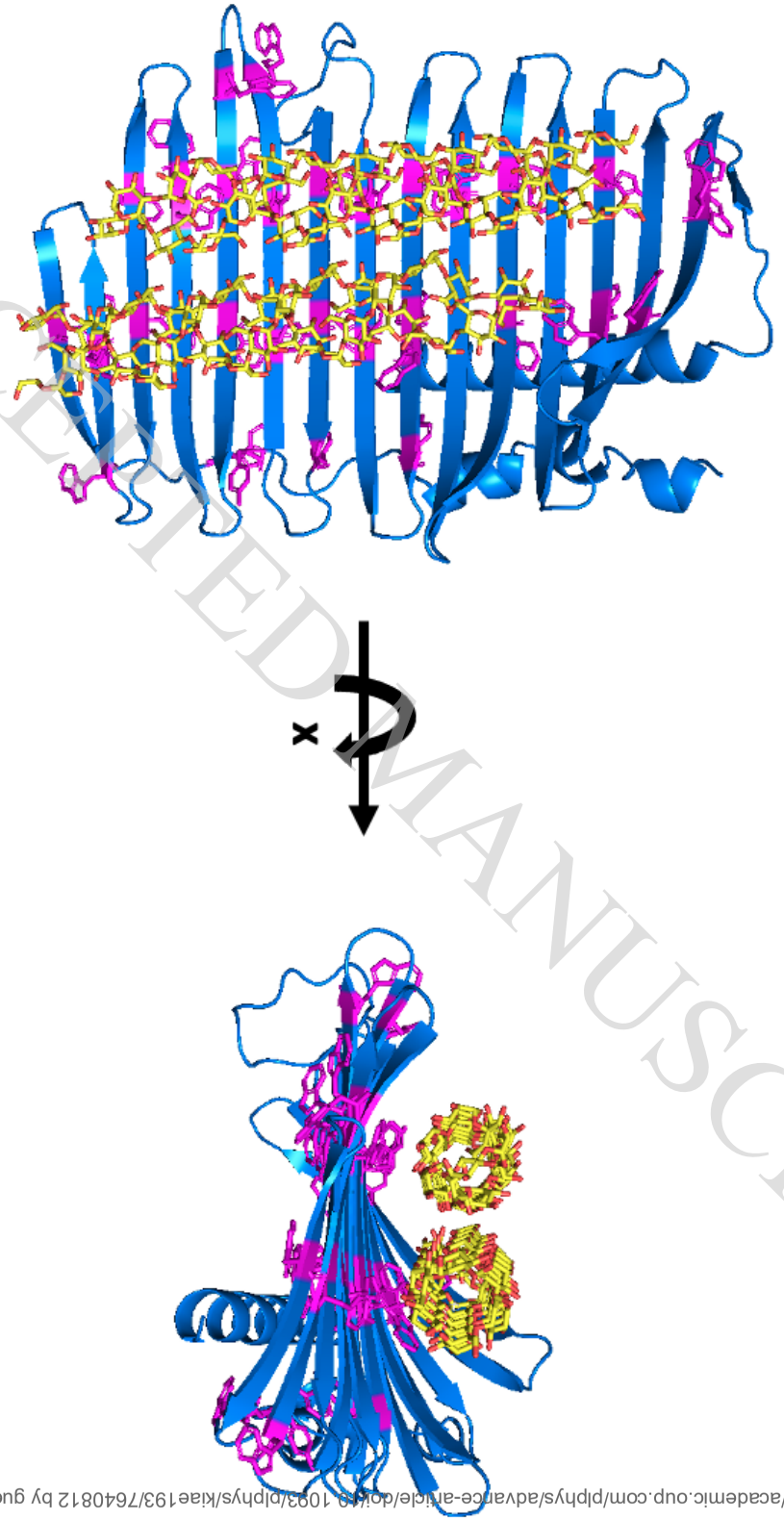

Parsed Citations

Ahmed Z, Tetlow IJ, Ahmed R, Morell MK, Emes MJ (2015) Protein-protein interactions among enzymes of starch biosynthesis in high-amylose barley genotypes reveal differential roles of heteromeric enzyme complexes in the synthesis of A and B granules. Plant Sci 233: 95-106
Google Scholar: Author Only Title Only Author and Title

Ball S, Guan HP, James M, Myers A, Keeling P, Mouille G, Buleon A, Colonna P, Preiss J (1996) From glycogen to amylopectin: a model for the biogenesis of the plant starch granule. Cell 86: 349-352
Google Scholar: Author Only Title Only Author and Title

Buleon A, Colonna P, Planchot V, Ball S (1998) Starch granules: structure and biosynthesis. Int J Biol Macromol 23: 85-112
Google Scholar: Author Only Title Only Author and Title

Crofts N, Abe N, Oitome NF, Matsushima R, Hayashi M, Tetlow IJ, Emes MJ, Nakamura Y, Fujita N (2015) Amylopectin biosynthetic enzymes from developing rice seed form enzymatically active protein complexes. J Exp Bot 66: 4469-4482
Google Scholar: Author Only Title Only Author and Title

David G, Perez J (2009) Combined sampler robot and high-performance liquid chromatography: a fully automated system for biological small-angle X-ray scattering experiments at the Synchrotron SOLEIL SWING beamline. Journal of applied crystallography 42: 9
Google Scholar: Author Only Title Only Author and Title

Delatte T, Trevisan M, Parker ML, Zeeman SC (2005) Arabidopsis mutants Atisa1 and Atisa2 have identical phenotypes and lack the same multimeric isoamylase, which influences the branch point distribution of amylopectin during starch synthesis. Plant J 41: 815-830
Google Scholar: Author Only Title Only Author and Title

Edelstein A, Amodaj N, Hoover K, Vale R, Stuurman N (2010) Computer control of microscopes using microManager. Curr Protoc Mol Biol Chapter 14: Unit14 20
Google Scholar: Author Only Title Only Author and Title

Feike D, Seung D, Graf A, Bischof S, Ellick T, Coiro M, Soyk S, Eicke S, Mettler-Altmann T, Lu KJ, Trick M, Zeeman SC, Smith AM (2016) The Starch Granule-Associated Protein EARLY STARVATION1 Is Required for the Control of Starch Degradation in Arabidopsis thaliana Leaves. Plant Cell 28: 1472-1489
Google Scholar: Author Only Title Only Author and Title

Franke D, Petoukov MV, Konarev PV, Panijkovich A, Tuukkanen A, Mertens HDT, Kikhney NR, Hajizadeh NR, Franklin JM, Jeffries CM, Svergun D (2017) ATSAS 2.8: a comprehensive data analysis suite for small-angle scattering from macromolecular solutions. Journal of applied crystallography 50: 1212-1225
Google Scholar: Author Only Title Only Author and Title

Helle S, Bray F, Verbeke J, Devassine S, Courseaux A, Facon M, Tokarski C, Rolando C, Szydlowski N (2018) Proteome Analysis of Potato Starch Reveals the Presence of New Starch Metabolic Proteins as Well as Multiple Protease Inhibitors. Front Plant Sci 9: 746
Google Scholar: Author Only Title Only Author and Title

Herrou J, Bompard C, Antoine R, Leroy A, Rucktooa P, Hot D, Huvent I, Locht C, Villeret V, Jacob-Dubuisson F (2007) Structure-based mechanism of ligand binding for periplasmic solute-binding protein of the Bug family. J Mol Biol 373: 954-964
Google Scholar: Author Only Title Only Author and Title

Hussain R, Javorfi T, Siligardi G, eds (2012) Spectroscopic analysis: synchrotron radiation circular dichroism., Vol 8. Elsevier, Amsterdam
Google Scholar: Author Only Title Only Author and Title

Hussain R, Longo E, Siligardi G (2018) UV-denaturation assay to assess protein photostability and ligand-binding interactions using the high photon flux of diamond B23 beamline for SRCD. . Molecules 23
Google Scholar: Author Only Title Only Author and Title

Imberty A, Chanzy H, Perez S, Buleon A, Tran V (1988) The double-helical nature of the crystalline part of A-starch. J Mol Biol 201: 365-378
Google Scholar: Author Only Title Only Author and Title

Jamme F, Bourquin D, Tawil G, Vikso-Nielsen A, Buleon A, Refregiers M (2014) 3D imaging of enzymes working in situ. Anal Chem 86: 5265-5270
Google Scholar: Author Only Title Only Author and Title

Jones G, Willett P, Glen RC, Leach AR, Taylor R (1997) Development and validation of a genetic algorithm for flexible docking. J Mol Biol 267: 727-748
Google Scholar: Author Only Title Only Author and Title

Jumper J, Evans R, Pritzel A, Green T, Figurnov M, Ronneberger O, Tunyasuvunakool K, Bates R, Zidek A, Potapenko A, Bridgland A, Meyer C, Kohl SAA, Ballard AJ, Cowie A, Romera-Paredes B, Nikolov S, Jain R, Adler J, Back T, Petersen S, Reiman D, Clancy E, Zielinski M, Steinegger M, Pacholska M, Berghammer T, Bodenstein S, Silver D, Vinyals O, Senior AW, Kavukcuoglu K, Kohli P, Hassabis D (2021) Highly accurate protein structure prediction with AlphaFold. Nature 596: 583-589
Google Scholar: Author Only Title Only Author and Title

Larson ME, Falconer DJ, Myers AM, Barb AW (2016) Direct Characterization of the Maize Starch Synthase IIa Product Shows Maltodextrin Elongation Occurs at the Non-reducing End. J Biol Chem 291: 24951-24960
Google Scholar: Author Only Title Only Author and Title

Liu C, Pfister B, Osman R, Ritter M, Heutinck A, Sharma M, Eicke S, Fischer-Stettler M, Seung D, Bompard C, Abt MR, Zeeman SC (2023) LIKE EARLY STARVATION 1 and EARLY STARVATION 1 promote and stabilize amylopectin phase transition in starch biosynthesis. Sci Adv 9: eadg7448
Google Scholar: Author Only Title Only Author and Title

Liu C, Pfister B, Osman R, Ritter M, Heutinck A, Sharma M, Eicke S, Fisher-Stettler M, Seung D, Bompard C, Abt MR, Zeeman SC (2023) LIKE EARLY STARVATION 1 and EARLY STARVATION 1 Promote and Stabilize Amylopectin Phase Transition in Starch Biosynthesis. Science Advances In press
Google Scholar: Author Only Title Only Author and Title

Malinova I, Mahto H, Brandt F, Al-Rawi S, Qasim H, Brust H, Hejazi M, Fettke J (2018) EARLY STARVATION1 specifically affects the phosphorylation action of starch-related dikinases. Plant J 95: 126-137
Google Scholar: Author Only Title Only Author and Title

Micsonai A, Wien F, Kernya L, Lee YH, Goto Y, Refregiers M, Kardos J (2015) Accurate secondary structure prediction and fold recognition for circular dichroism spectroscopy. Proc Natl Acad Sci U S A 112: E3095-3103
Google Scholar: Author Only Title Only Author and Title

Miles AJ, Janes RW, Brown A, Clarke DT, Sutherland JC, Tao Y, Wallace BA, Hoffmann SV (2008) Light flux density threshold at which protein denaturation is induced by synchrotron radiation circular dichroism beamlines. J Synchrotron Radiat 15: 420-422
Google Scholar: Author Only Title Only Author and Title

Miles AJ, Wallace BA (2018) CDtoolX, a downloadable software package for processing and analyses of circular dichroism spectroscopic data. Protein Sci 27: 1717-1722
Google Scholar: Author Only Title Only Author and Title

Miles AJ, Wien F, Wallace BA (2004) Redetermination of the extinction coefficient of camphor-10-sulfonic acid, a calibration standard for circular dichroism spectroscopy. Anal Biochem 335: 338-339
Google Scholar: Author Only Title Only Author and Title

Myers AM, Morell MK, James MG, Ball SG (2000) Recent progress toward understanding biosynthesis of the amylopectin crystal. Plant Physiol 122: 989-997
Google Scholar: Author Only Title Only Author and Title

Pérez S, Bertoft E (2010) The molecular structures of starch components and their contribution to the architecture of starch granules: A comprehensive review. . Starch-Stärke 62: 389-420
Google Scholar: Author Only Title Only Author and Title

Petoukhov MV, Svergun DI (2005) Global rigid body modeling of macromolecular complexes against small-angle scattering data. Biophys J 89: 1237-1250
Google Scholar: Author Only Title Only Author and Title

Pfister B, Lu KJ, Eicke S, Feil R, Lunn JE, Streb S, Zeeman SC (2014) Genetic Evidence That Chain Length and Branch Point Distributions Are Linked Determinants of Starch Granule Formation in Arabidopsis. Plant Physiol 165: 1457-1474
Google Scholar: Author Only Title Only Author and Title

Pfister B, Zeeman SC (2016) Formation of starch in plant cells. Cell Mol Life Sci 73: 2781-2807
Google Scholar: Author Only Title Only Author and Title

Refregiers M, Wien F, Ta HP, Premvardhan L, Bac S, Jamme F, Rouam V, Lagarde B, Polack F, Giorgetta JL, Ricaud JP, Bordessoule M, Giuliani A (2012) DISCO synchrotron-radiation circular-dichroism endstation at SOLEIL. J Synchrotron Radiat 19: 831-835
Google Scholar: Author Only Title Only Author and Title

Sawada T, Nakamura Y, Ohdan T, Saitoh A, Francisco PB, Jr., Suzuki E, Fujita N, Shimonaga T, Fujiwara S, Tsuzuki M, Colleoni C, Ball S (2014) Diversity of reaction characteristics of glucan branching enzymes and the fine structure of alpha-glucan from various sources. Arch Biochem Biophys 562: 9-21
Google Scholar: Author Only Title Only Author and Title

Schindelin J, Arganda-Carreras I, Frise E, Kaynig V, Longair M, Pietzsch T, Preibisch S, Rueden C, Saalfeld S, Schmid B, Tinevez

JY, White DJ, Hartenstein V, Eliceiri K, Tomancak P, Cardona A (2012) Fiji: an open-source platform for biological-image analysis. Nat Methods 9: 676-682
Google Scholar: Author Only Title Only Author and Title

Singh A, Compart J, Al-Rawi SA, Mahto H, Ahmad AM, Fettke J (2022) LIKE EARLY STARVATION 1 alters the glucan structures at the starch granule surface and thereby influences the action of both starch-synthesizing and starch-degrading enzymes. Plant J 111: 819-835
Google Scholar: Author Only Title Only Author and Title

Streb S, Delatte T, Umhang M, Eicke S, Schorderet M, Reinhardt D, Zeeman SC (2008) Starch granule biosynthesis in Arabidopsis is abolished by removal of all debranching enzymes but restored by the subsequent removal of an endoamylase. Plant Cell 20: 3448-3466
Google Scholar: Author Only Title Only Author and Title

Tawil G, Jamme F, Refregiers M, Vikso-Nielsen A, Colonna P, Buleon A (2011) In situ tracking of enzymatic breakdown of starch granules by synchrotron UV fluorescence microscopy. Anal Chem 83: 989-993
Google Scholar: Author Only Title Only Author and Title

Tsai CY (1974) The function of the waxy locus in starch synthesis in maize endosperm. Biochem Genet 11: 83-96
Google Scholar: Author Only Title Only Author and Title

Waight TA, Kato LK, Donald AM, Gidley MJ, Clarke CJ, Riekel C (2000) Side-Chain Liquid-Crystalline Model for Starch. Starch-Stärke 52: 450-460
Google Scholar: Author Only Title Only Author and Title

Wattebled F, Dong Y, Dumez S, Delvalle D, Planchot V, Berbezy P, Vyas D, Colonna P, Chatterjee M, Ball S, D'Hulst C (2005) Mutants of Arabidopsis lacking a chloroplastic isoamylase accumulate phytoglycogen and an abnormal form of amylopectin. Plant Physiol 138: 184-195
Google Scholar: Author Only Title Only Author and Title

Xie Y, Barb AW, Hennen-Bierwagen TA, Myers AM (2018) Direct Determination of the Site of Addition of Glucosyl Units to Maltooligosaccharide Acceptors Catalyzed by Maize Starch Synthase I. Front Plant Sci 9: 1252
Google Scholar: Author Only Title Only Author and Title

Zeeman SC, Umemoto T, Lue WL, Au-Yeung P, Martin C, Smith AM, Chen J (1998) A mutant of Arabidopsis lacking a chloroplastic isoamylase accumulates both starch and phytoglycogen. Plant Cell 10: 1699-1712
Google Scholar: Author Only Title Only Author and Title

Ziegler GR, Creek JA, Runt J (2005) Spherulitic crystallization in starch as a model for starch granule initiation. Biomacromolecules 6: 1547-1554
Google Scholar: Author Only Title Only Author and Title